Propagation of Highly Chirped Pulses in Fiber-Optic Communications Systems

S. T. Cundiff, B. C. Collings, L. Boivin, M. C. Nuss, K. Bergman, W. H. Knox, and S. G. Evangelides, Jr.

Abstract— **The propagation of strongly chirped pulses in an amplified fiber-optic communications system is experimentally investigated. Spectral narrowing of the pulses is observed. The narrowing is attributed to interplay between the initial chirp and the nonlinearity in the transmission line. Four-wave mixing (FWM) between wavelength channels is found to be similar to that for unchirped nonreturn-to-zero (NRZ) pulses. Low error rate transmission over 720 km is achieved using these chirped pulses, which are generated by a transmitter based on a mode-locked fiber laser.**

Index Terms— **Mode locked lasers, nonlinear optics, optical fiber communication, optical fiber dispersion, optical fiber lasers.**

I. Introduction

THE propagation of optical pulses through an optically amplified transmission line has been the subject of much study since the invention of erbium-doped fiber amplifiers (EDFA's) [1], [2]. These studies have concentrated on two data formats, nonreturn-to-zero (NRZ) and solitons (which are return-to-zero (RZ) pulses). A wide range of intermediate formats have also been considered to a lesser extent. NRZ is used because it requires minimum transmitter and receiver bandwidth. At lower data rates, detrimental transmission effects, such as group-velocity dispersion (GVD) and fiber nonlinearity, can be linearly compensated or are negligible for NRZ format data. However, at higher data rates and with the deployment of wavelength division multiplexed (WDM) systems, countermeasures must be employed to minimize the impact of these detrimental effects on system performance [3]. Soliton transmission, in contrast, uses these two effects to balance and compensate each other [4]. Both transmission schemes also suffer from higher order effects [dispersion slope (DS), four-wave mixing (FWM), amplifier spontaneous emission (ASE) noise, etc.].

Here we present a study of the propagation of pulses that are neither conventional NRZ nor solitons. They are highly chirped RZ pulses. These pulses are naturally generated by a WDM transmitter that utilizes the broad optical bandwidth of a modelocked laser producing subpicosecond pulses. We denote this technique as chirped-pulse WDM (CPWDM) [5]. The focus of this paper is on the physics and systems impact of using highly chirped pulses. The CPWDM technique has several attractive features, including use of only a single laser and a single modulator. It has produced a record number of WDM channels (recent results have exceeded 300) [6]. It can act as an optical TDM to WDM converter. In its basic configuration it is not as spectrally efficient as other techniques, however interleaving schemes can improve this. The relative balance of its advantages and disadvantages remains to be seen.

Chirp has generally been avoided in NRZ systems because it increases the optical bandwidth and hence the effects of GVD. Although recently, phase modulation prior to launch, which is similar to chirp, has been used as a countermeasure against the deleterious effects of fiber nonlinearity [7].

It is generally expected that RZ pulses should suffer greater penalties due to fiber nonlinearity [8] than NRZ pulses because their shorter duty cycle leads to a greater peak power (for the same energy per pulse). In particular, self-phase modulation (SPM) on the rising and falling edges of a pulse will result in spectral broadening. We show that, on the contrary, the SPM results in spectral narrowing of the optical spectrum for chirped pulses. This only occurs if the transmitter generates pulses with the correct chirp. A numerical simulation is presented that reproduces the spectral narrowing. The spectral narrowing is relative to the input pulses, the narrowed spectrum may still be larger than that obtained from other schemes.

In addition to spectral reshaping due to SPM, fiber nonlinearity can cause interchannel interference in a WDM system due to FWM. The impact of FWM on CPWDM is explored. While the degradation and limits imposed by FWM are highly dependent upon the transmission system configuration, some general conclusions can be drawn. In particular, for systems employing CPWDM in its basic format, FWM is a minimal effect as there is no temporal overlap between the pulses launched in different wavelength channels. However, near zero GVD, third-order dispersion (TOD) can result in overlap during propagation.

The capacity of a CPWDM system can be increased by interleaving the output of multiple CPWDM transmitters, in which case there is temporal overlap between wavelength channels. The pulses are still highly chirped, which is the distinguishing feature as compared to other WDM formats. In this case, temporal overlap will occur and the implications of FWM become more complex and dependent upon system parameters. Then the issues are similar to those for conventional nonsoliton WDM systems.

Manuscript received July 6, 1998; revised January 8, 1999.

S. T. Cundiff was with Bell Laboratories, Lucent Technologies, Holmdel, NJ 07733 USA. He is now with JILA/University of Colorado, Boulder CO 80309-0440 USA.

B. C. Collings, L. Boivin, M. C. Nuss, and W. H. Knox are with Bell Laboratories, Lucent Technologies, Holmdel, NJ 07733 USA.

K. Bergman is with the Electrical Engineering Department, Princeton University, Princeton, NJ 08544 USA.

S. G. Evangelides, Jr. is with Submarine Systems International Laboratories, Holmdel, NJ 07733 USA.

Publisher Item Identifier S 0733-8724(99)02689-4.

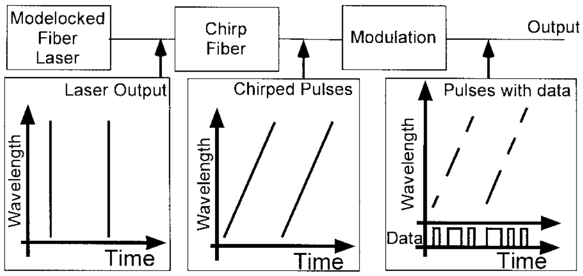

Fig. 1. Schematic of CPWDM transmitter. The wavelength versus time relationship is shown at several points.

Finally, we are experimentally able to obtain low error rate transmission over 720 km using the chirped pulses produced by a CPWDM transmitter. Low error rate transmission is only occurs for the correct sign of the initial chirp, where the spectral integrity of the individual channels is preserved by the nonlinear spectral narrowing. For the opposite sign, spectral broadening occurs and low error rate transmission cannot be obtained due to the rapid loss of the spectral integrity.

We will first review the CPWDM transmitter, the resulting transmission format and present the characteristics of the transmission line. Then we will present the results that are sensitive to the transmission line nonlinearity, first showing the spectral narrowing, followed by an examination of FWM. Finally, the bit-error-rate measurements showing low error-rate transmission will be presented.

II. Transmitter and Transmission Format

The CPWDM transmitter [5], [6], [9] is shown schematically in Fig. 1. It consists of a modelocked fiber laser, a length of fiber to impose a linear chirp on the pulse and an intensity modulator for encoding data on the resulting chirped pulses. The lower panels show the time-wavelength relationship. At the output of the laser, all wavelength components are coincident in time, after the chirp fiber they are sequential in time within a given pulse. If the modulator is running at N times the laser repetition rate, then every Nth bit modulates the same wavelength. With appropriate bit-interleaving, a unique data stream is encoded on each wavelength. CPWDM is one example of spectral slicing in a WDM transmitter [10]–[12].

The data format produced by a CPWDM transmitter differs from that produced by conventional WDM techniques. In Fig. 2, we show the output waveform of a CPWDM transmitter divided up into wavelength and time slots. This makes the differences clear: the pulses for each wavelength are RZ with a low duty factor and the pulses at different wavelengths do not overlap with each other within a time slot. It is interesting to realize that the data applied to the modulator is actually NRZ, and hence so is the spectrally integrated intensity emitted by the transmitter in the absence of any other spectral filtering at the transmitter. It is only upon separation into individual wavelength channels by the receiver optical filter that the pulses become RZ. For the transmission experiments, we found it advantageous to narrow the launch spectrum of each channel by applying a coarse spectral comb filter, in this case the pulses are RZ, both spectrally integrated and within a channel. The duty factor of each channel is determined by the modulation rate, i.e., it is $1/N$. The channel spacing is determined by a combination of the modulation rate and the total dispersion of the chirp fiber. The absolute channel wavelength is determined by the time position of the data stream applied to the modulator in relation to the arrival time of the pulse. For a given transmitter configuration, the channel spacing is fixed, while the wavelength can easily be adjusted by changing that relationship.

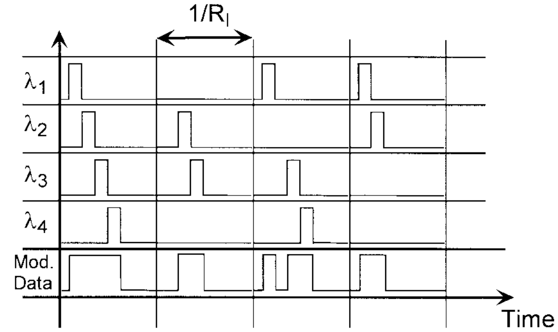

Fig. 2. Time slot diagram of the data for four of the wavelength channels generated by a CPWDM transmitter. The vertical lines denote time slots separated by the time between laser pulses, i.e, $1/R_l$ where R_l is the laser repetition rate. The bottom section shows the data applied to the modulator.

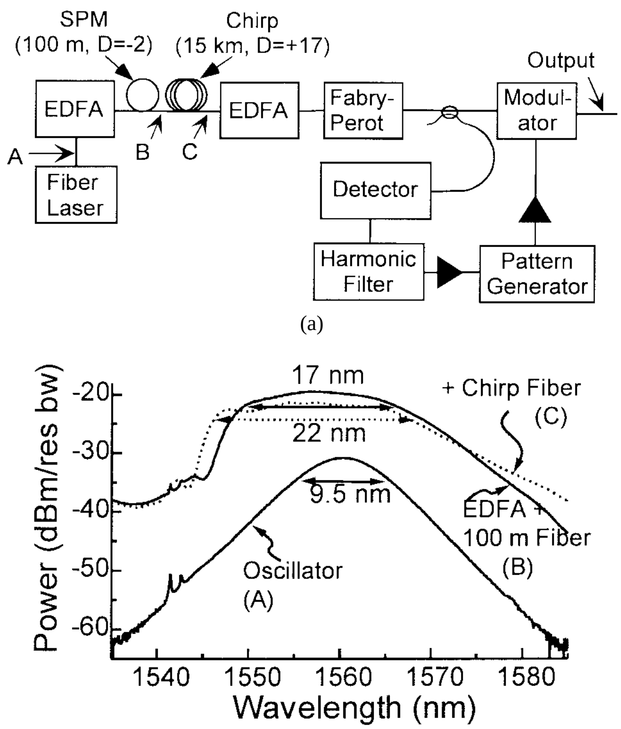

Fig. 3. (a) Diagram of CPWDM transmitter components and (b) spectra at several points in the transmitter. Letters denote positions where spectra were taken.

Fig. 3 shows a detailed diagram of the CPWDM transmitter. Several intermediate optical spectra are also shown.

A short cavity erbium-ytterbium fiber laser [13] is used as the optical oscillator in the CPWDM transmitter. The laser is passively mode-locked using a semiconductor saturable-Bragg reflector at one end of the cavity [14]. The other end is a dielectric stack coated directly onto a fiber ferrule; it serves as an output coupler. The Er/Yb gain fiber is pumped through the output coupler at 980 nm by a telecommunications qualified, 90 mW diode. The fiber laser operates at a repetition rate of 155.5 MHz, which determines the bit rate per channel.

The direct output spectrum from the fiber laser does not overlap well with or fill the EDFA passband of the transmission system (described in the next section). To remedy this, we use SPM in low dispersion fiber to increase the bandwidth. This is accomplished by amplifying the output of the fiber laser in a dispersion compensated EDFA. The amplifier is slightly over compensated, resulting in an output pulse with a slight residual anomalous chirp. This is launched into 100 m of low, normal dispersion fiber ($D \sim -2$ ps/km/nm). The spectrum resulting from SPM in nearly ideal for this application, it is relatively flat with 3 dB points that correspond very closely to those of the amplifier chain.

The spectrally broadened output pulses are linearly chirped by passage through 15 km of standard single-mode fiber ($D =$ 17 ps/nm/km). As this chirp fiber has anomalous dispersion, the pulses recompress in the beginning and undergoes further SPM, additionally broadening the spectrum. The power is insufficient for significant soliton effects to occur in the chirp fiber. The channels are spectrally defined by a low-finesse Fabry–Perot. An InGaAsP electroabsorption modulator [15] encodes the data on the channels. The modulator is driven at 36 times the laser repetition rate (5.58 GHz). The spacing of the Fabry–Perot is carefully adjusted so that its free spectral range matches the channel spacing determined by the combination of the modulation rate and chirp. In this setup, the laser acts as the master clock. The clock that drives the pattern generator is derived by using a fast photodiode to detect the train of pulses transmitted through the Fabry–Perot and filtering out the 36th harmonic from the RF spectrum. This guarantees the correct phase relationship between the spectrum and data.

With a modulation rate that is 36 times the laser repetition rate, the transmitter can produce 36 wavelength channels. However complete utilization of all of these channels is only possible for a optical spectrum with a perfect top hat profile. To prevent temporal overlap of wavelengths near the red end of the spectrum with those at the blue end, the pulse must be chirped less than would result in complete use of all the channels. Consequently we only use 18 of the 36 channels in our propagation experiment. These 18 channels are chosen to fill the transmission line amplifier passband.

III. Transmission Line

The transmission line has a total length of 720 km and consists of 16 spans (Fig. 4). Each span has an EDFA, ~2 km of SMF and 43 km of dispersion shifted fiber for a net dispersion of approximately 0.6 ps/nm/km at 1555 nm. Each EDFA has two gain segments and a fiber grating filter to suppress the 1535 nm erbium peak. A single adjustable gain-flattening filter is installed at the halfway point of the transmission line. The amplified spontaneous emission spectrum of the transmission line is shown in Fig. 4 as an approximate measure of its gain spectrum (the amplifiers are not strongly saturated).

As the GVD, including GVD slope due to TOD, is important for determining if there is overlap between pulses

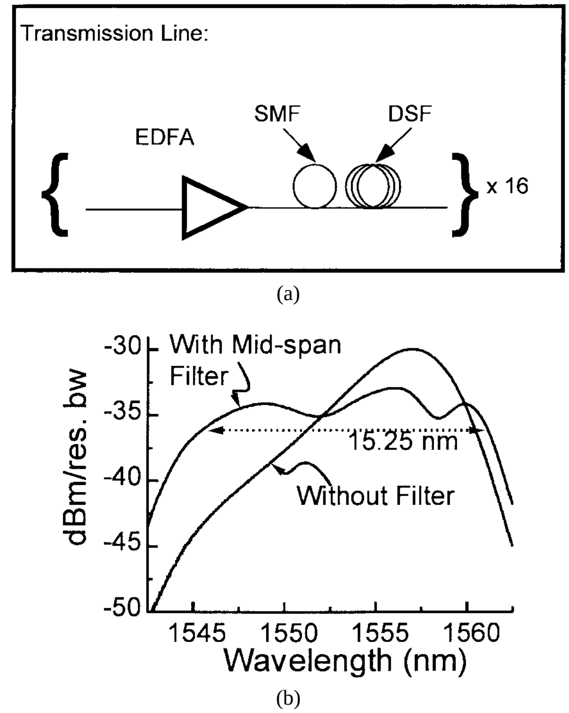

Fig. 4. (a) Schematic of transmission line and (b) the ASE spectrum (with and without gain flattening filter).

from neighboring frames (where a frame is defined as the set of bits, one per channel, that are created from a single pulse from the fiber laser), we carefully characterized the transmission line using a time-of-flight measurement. The results are presented in Fig. 5. Based on these results, we can extract the transmission line characteristics and find that it has a zero dispersion wavelength, $\lambda_0 = 1549.2$ nm and dispersion slope, $D' = 0.075$ ps/nm^2-km. Both parameters are consistent with the design of the transmission line. The results show that there is some interframe overlap between well separated wavelength channels due to dispersion. Reducing this would require adjustment of λ_0 such that it lay within the wavelength band of interest. However, this would have the detrimental effect of causing intraframe overlap between adjacent wavelength channels. This, in turn, could result in significant FWM (see Section VI), hence the choice of λ_0.

IV. Spectral Narrowing: Experiment

The combination of large channel optical bandwidth and low duty cycle pulses produced by CPWDM might be expected to result in strong transmission impairments due to spectral broadening resulting from SPM. Surprisingly, we observe just the opposite. In Fig. 6 we compare the channel spectra before and after propagation through the 720 km transmission line. For this figure, the channels are simply defined by the Fabry–Perot and no data-modulation is applied (there is a pulse in every time and wavelength slot). Spectral narrowing is evident.

The narrowing is clearly due to nonlinearity in the transmission line as it depends on the launch power (note that the early EDFA's in the transmission line are not operating in saturation, hence the launch power determines the propagating intensity). This is shown in Fig. 7.

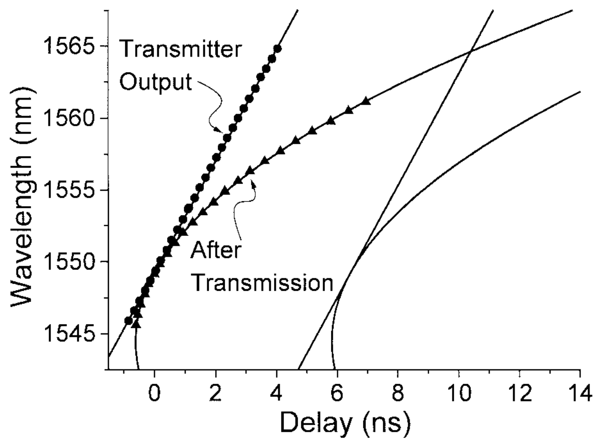

Fig. 5. Time-of-flight measurement of GVD. Dots are measured at output of transmitter, triangles after 720 km propagation. Lines are a parabolic fit to the data. Second set of lines are shifted the time between data pulses to show how dispersion can result in overlap between channels.

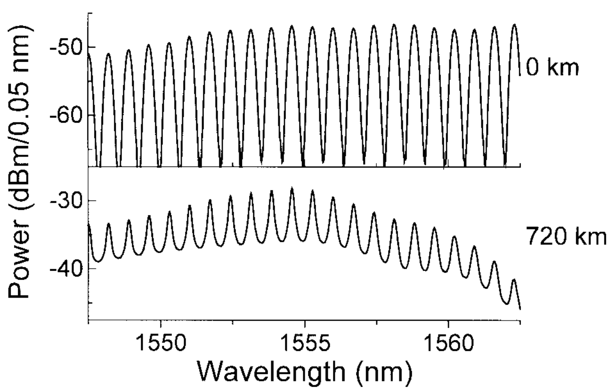

Fig. 6. Measured channel spectra before and after propagation, showing spectral narrowing. The launced power was -44 to -46 dBm per channel, the average power in the transmission line was ~ -20 dBm. The contrast reduction is due to ASE.

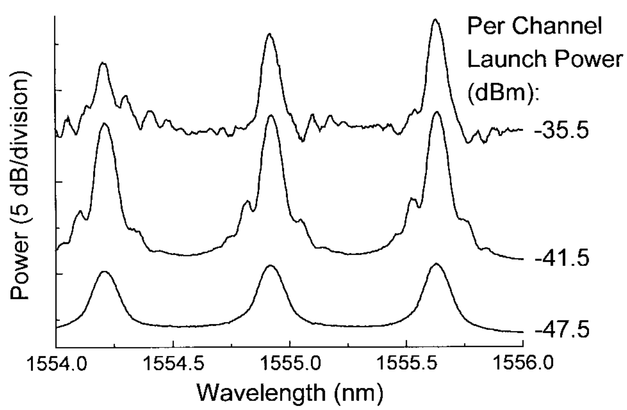

Fig. 7. Transmitted channel spectra for various launch powers showing that the narrowing is clearly power dependent.

The spectral narrowing also depends on the initial chirp generated by the CPWDM transmitter. In Fig. 8 we show that the effect of the nonlinearity changes from narrowing to broadening if the sign of the initial chirp is changed (by using high normal dispersion fiber in the transmitter). The magnitude of the net chirp is approximately the same in both results displayed here, only the sign is changed.

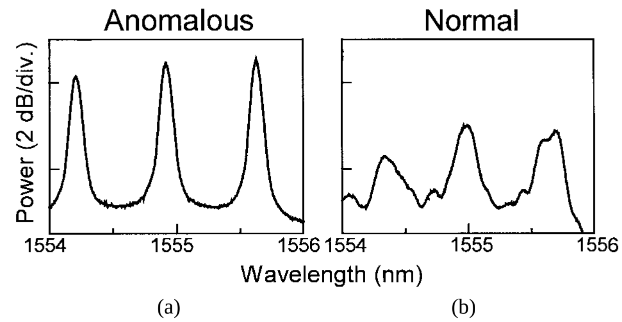

Fig. 8. Comparison of transmitted spectra for (a) anomalous dispersion and (b) normal dispersion chirp fiber in the transmitter. Narrowing is clearly evident in (a) while broadening occurs in (b).

The origin of the spectral narrowing can be understood by considering how SPM affects a chirped pulse with a square or super-Gaussian profile, i.e., not the pulse profile generated by the Fabry–Perot, (Fig. 9). The nonlinear index only varies on the rising and falling edges of the pulse [Fig. 9(a) and (b)], resulting in a red shift of the front and blue shift of the back. When the pulses are initially chirped using normal dispersion fiber, so that long and short wavelengths occur at the front and back of the pulses, respectively, the corresponding red and blue shifts generate new frequencies, causing spectral broadening [Fig. 9(c)]. However, when anomalous dispersion fiber is used in the transmitter, SPM redistributes the energy toward the center of the spectrum and produces narrowing [Fig. 9(d)]. Numerical results, for a symmetrized split-step propagation model, provide good agreement with experimental results [Fig. 9(e) and (f)]. The model does not include ASE, gain/absorption or transmission line dispersion. Nonlinear spectral narrowing has previously been observed at 850 nm [16]. In a very qualitative sense, the narrowing can be thought of as being analogous to the formation of a soliton, i.e. GVD and SPM are acting to balance each other, however we have spatially separated the dispersive and nonlinear parts.

V. Four-Wave-Mixing

Due to the Kerr nonlinearity of optical fiber, copropagating pulses of differing frequencies undergo FWM, causing the transfer of power into new optical frequencies [3], [8]. This effect can impose a significant power limitation upon WDM transmission systems because it is an intensity dependent cross-talk process. The most detrimental FWM process occurs when three equally spaced (in optical frequency) channels (all with “ones” present) mix, generating an electric field at the center channel frequency. This generated field, with an optical phase dependent upon the phases of the two outer channels, coherently interferes with the existing electric field in the center channel. This small generated field can cause a very large change in the resulting intensity of the sum of fields. This interference manifests itself as eye closure. Several schemes can be implemented to suppress or avoid this effect [3].

For the standard CPWDM transmitter, FWM is largely avoided due to the launched time-wavelength relationship (Fig. 5). Contrary to conventional systems, there is no temporal overlap between the bits of any wavelength channels. If the transmission line consists of fiber with significant GVD

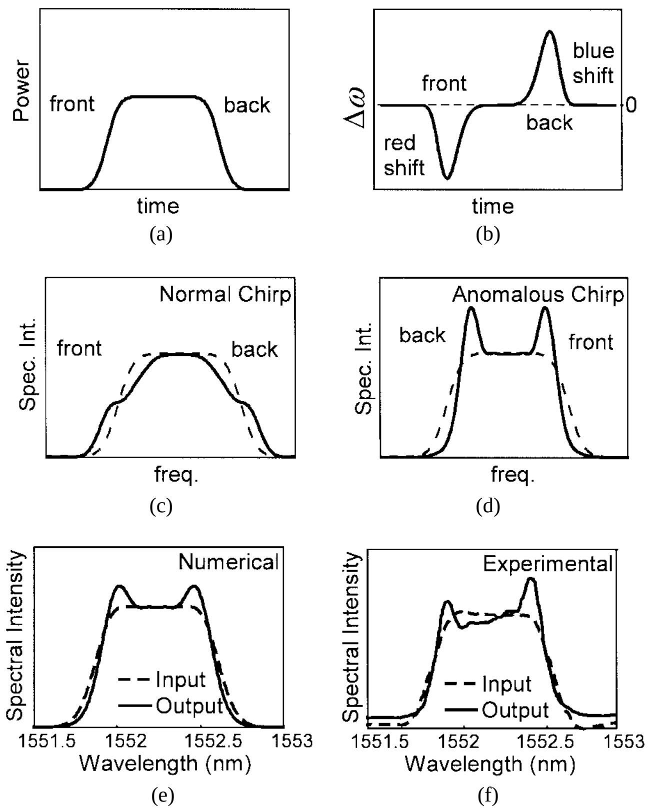

Fig. 9. (a)–(d) Schematic showing how SPM affects a highly chirped, square pulse. (a) Input pulse. (b) The new frequency components generated by SPM. (c) Broadening or (d) narrowing of the spectrum depends on the sign of the initial chirp. In (c) and (d), the dashed line is the initial pulse, solid includes SPM. (e) and (f) Comparison of a numerical calculation including SPM and initial chirp (e) to experimental results (f).

of the same sign as the chirp fiber, the temporal separation between adjacent wavelength channels will increase, further avoiding temporal overlap and FWM. After significant dispersive propagation, this may lead to interframe overlap as each frame is chirped to a duration greater than the period between pulses (Fig. 5). This overlap should not cause significant FWM since the overlapping channels will have large frequency separations. However, for very large propagation distances, the frequency separation between overlapping channels becomes similar to the channel spacing and the FWM efficiency increases. Then, the bits of each channel fill each bit time-slot so that each channel approximates a NRZ waveform.

If the transmission fiber has large GVD and a sign opposite to that of the chirp fiber, propagation will remove the linear chirp produced by the CPWDM transmitter. As the magnitude of the total transmission line GVD approaches that of the chirp fiber, temporal overlap will begin to occur. Also, due to the RZ nature of the pulses, the FWM efficiency will be large due to the higher peak power, in comparison to an equivalent NRZ pulse (for the same energy per bit).

A transmission line with near zero GVD and no TOD preserves the linear relationship between wavelength and time, thus avoiding FWM. However, TOD can cause curvature of the wavelength-time relationship with a vertex at λ_0 (Fig. 5.). Thus, near λ_0, temporal overlap and FWM will occur after significant propagation. This problem is intensified since the

TABLE I
CHANNEL BER AND RECEIVED POWER FOR BER $<10^{-9}$ OPERATION

		Back-to-Back		720 km	
Channel	λ	I_{rec} (dBm)	BER	I_{rec} (dBm)	BER
8	1551.2	-43.82	8×10^{-10}	-42.03	8×10^{-10}
11	1553.3	-43.31	1×10^{-9}	-41.24	6×10^{-10}
18	1558.3	-43.23	5×10^{-10}	-41.24	8×10^{-10}

degree of phase matching of these channels will be high, leading to a large FWM efficiency.

To increase the capacity of a CPWDM system, while still using available high speed modulators (<20 GHz), a bit interleaved scheme has been proposed. By time-interleaving independent CPWDM waveforms, the bit rate of each channel can be increased with additional modulators. However, temporal overlap is then present between channels. The frequency separation between overlapping channels is dependent on the interleaving ratio (the number of channels divided by the number of interleaved waveforms). As this ratio approaches unity, the frequency separation between overlapping channels approaches the frequency separation between adjacent wavelength channels. Under these conditions, the bandwidth is fully utilized and each wavelength channel approximates a NRZ waveform. Short of this condition, each channel is approximated as a RZ waveform with a duty cycle equal to the interleaving ratio.

Experiments and theoretical simulations show that the chirped nature of the pulses does not significantly impact the FWM efficiency. Thus, the effects of FWM on interleaved systems with low interleaving ratios are similar to the penalties experienced by an analogous conventional RZ or NRZ WDM system. Therefore, the high local GVD maps currently used to suppress the effects of FWM may be expected to be equally effective in these interleaved CPWDM systems.

VI. BIT ERROR MEASUREMENTS

To verify that the observed spectral narrowing actually improves system performance, we performed (BER) measurements at 155 Mb/s/channel on three of the 18 channels. Two are near the center, the other on the edge of the amplifier passband. To perform these measurements a pseudo-random bit stream (PRBS) was generated, interleaved with an offset and loaded into the pattern generator. The offset means that the PRBS's for adjacent channels are not correlated. Each PRBS had a length of $2^{15}-1$ bits. The received wavelength channels were spectrally separated using a bulk optic grating filter with a 0.25 nm bandpass prior to detection with a fast photodiode. Clock recovery was performed using a phase locked loop.

The results are summarized in Table I, comparing the back-to-back BER to that for 720 km transmission. For these measurements a chirp fiber with anomalous dispersion was used in the transmitter. All 18 channels were operating. It was possible to achieve low error rate transmission on all three measured channels (BER $\leq 10^{-9}$). The propagation over 720 km resulted in a power penalty of approximately 2 dB. Fig. 10(a) shows an eye-diagram for the transmitted data.

For the opposite sign of chirp from the transmitter, low error rate transmission was not possible independent of the

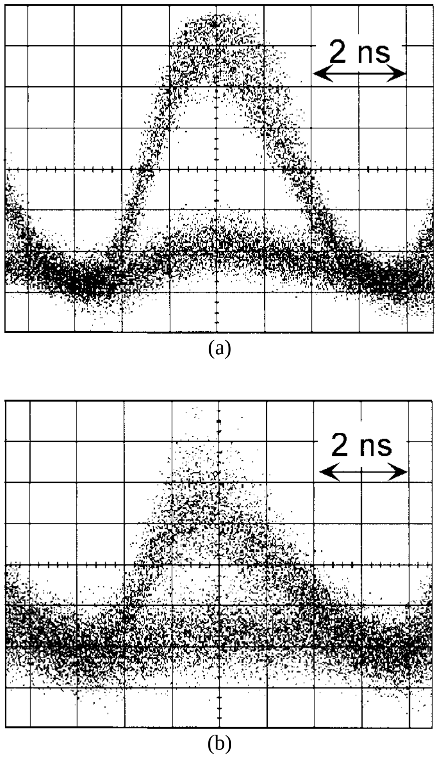

Fig. 10. Eye diagrams after 720 km transmission. For (a), a chirp fiber with anomalous dispersion was used in the transmitter, while for (b), a chirp with normal dispersion was used.

launch power. In this case, the spectral broadening resulted in complete eye closure, as shown in Fig. 10(b).

Measurements showed that FWM did not have a significant impact on the BER measurements. It may become more significant for a system that uses interleaving to increase the aggregate capacity.

VII. Summary

We have presented the results of transmission experiments using highly chirped pulses. For these measurements, the pulses were generated using a CPWDM transmitter, although the results are generally applicable to any source of chirped pulses. Our measurements showed that interplay between the initial chirp and transmission-line nonlinearity results in spectral narrowing of the pulses' optical spectra. We are able to obtain low error rate transmission over an amplified 720 km transmission line. FWM is not found to be significant for the transmission line configuration that we used.

Acknowledgment

The authors would like to acknowledge helpful discussions with A. R. Chraplyvy.

References

[1] E. Desurvire, *Erbium-Doped Fiber Amplifiers*. New York: Wiley, 1994.
[2] I. P. Kaminow and T. L. Koch, Eds. *Optical Fiber Telecommunications IIIA & B*. San Diego, CA: Academic, 1997.
[3] F. Forghieri, R. W. Tkach, and A. R. Chraplyvy, "Fiber nonlinearities and their impact on transmission systems," in *Optical Fiber Telecommunications IIIA*, I.P. Kaminow and T.L. Koch, Eds. San Diego, CA: Academic, 1997, pp. 196–264.
[4] L. F. Mollenauer, J. P. Gordon, and P. Mamyshev, "Soliton transmission," in *Optical Fiber Telecommunications IIIA*, I. P. Kaminow and T. L. Koch, Eds. San Diego, CA: Academic, 1997.
[5] M. C. Nuss, W. H. Knox, and U. Koren, "Scalable 32 Channel chirped-pulse WDM source," *Electron. Lett.*, vol. 32, pp. 1311–1312, 1996.
[6] L. Boivin, M. C. Nuss, W. H. Knox, and J. B. Stark, "206-channel chirped-pulse wavelength-division multiplexed transmitter," *Electron. Lett.*, vol. 33, pp. 827–829, 1997.
[7] N. S. Bergano, C. R. Davidson, and F. Heismann, "Bit-synchronous polarization and phase modulation improves the performance of optical amplifier transmission systems." in *Proc. Opt. Fiber Commun., Opt. Soc. Amer.*, San Jose, CA, 1996.
[8] G. P. Agrawal, *Nonlinear Fiber Optics*, 2nd ed. San Diego, CA: Academic, 1995.
[9] S. T. Cundiff, W. H. Knox, and M. C. Nuss, "Active feed-forward channel equalization for chirped pulse wavelength division multiplexing," *Electron. Lett.*, vol. 33, pp. 10–11, 1997.
[10] J. S. Lee, Y. C. Chung, and D. J. DiGiovanni, "Spectrum-sliced fiber amplifier light source for multichannel WDM applications," *IEEE Photon. Technol. Lett.*, vol. 5, pp. 1458–1461, 1993.
[11] E. A. DeSouza, M. C. Nuss, W. H. Knox, and D. A. B. Miller, "Wavelength-division multiplexing with femtosecond pulses," *Opt. Lett.*, vol. 20, pp. 1166–1168, 1995.
[12] K.-Y. Liou, J. B. Stark, U. Koren, E. C. Burrows, J. L. Zyskind, and K. Dreyer, "System performance of an eight-channel WDM local access network employing a spectrum-sliced and delay-line-multiplexed LED source," *IEEE Photon. Technol. Lett.*, vol. 9, pp. 696–698, 1997.
[13] B. C. Collings, K. Bergman, S. T. Cundiff, S. Tsuda, J. N. Kutz, M. Koch, and W. H. Knox, "Short cavity erbium/ytterbium fiber lasers mode-locked with a saturable Bragg reflector," *IEEE J. Select. Top. Quantum Electron.*, vol. 3, pp. 1065–1075, 1997.
[14] S. Tsuda, W. H. Knox, E. A. de Souza, W. Y. Jan, and J. E. Cunningham, "Low loss intracavity AlAs/AlGaAs Saturable Bragg Reflector for femtosecond mode-locking in solid state lasers," *Opt. Lett.*, vol. 20, pp. 1406–1408, 1995.
[15] U. Koren, R. Micheal, B. I. Miller, M. G. Yound, M. Chien, H. H. Yaffe, G. Raybon, and K. Dreyer, "Electro absorption modulators with passive waveguide spot size converters," *Electron. Lett.*, vol. 33, pp. 827–829, 1997.
[16] M. Oberthaler and R. A. Höpfel, "Special narrowing of ultrashort laser pulses by self-phase modulation in optical fibers," *Appl. Phys. Lett.*, vol. 63, pp. 1017–1019, 1993.

S. T. Cundiff, photograph and biography not available at the time of publication.

B. C. Collings, photograph and biography not available at the time of publication.

L. Boivin, photograph and biography not available at the time of publication.

M. C. Nuss, photograph and biography not available at the time of publication.

K. Bergman, photograph and biography not available at the time of publication.

W. H. Knox, photograph and biography not available at the time of publication.

S. G. Evangelides, Jr., photograph and biography not available at the time of publication.